

SUPPORTING INFORMATION

Supporting Information

Incorporating Au₁₁ Nanocluster on MoS₂ Nanosheet Edges for Promoting Hydrogen Evolution Reaction at the Interface

Saniya Gratiious,^a Arun Karmakar,^{b,‡} Dhirendra Kumar,^{c,‡} Subrata Kundu,^b Sudip Chakraborty,^c and Sukhendu Mandal^{a}*

^a School of Chemistry, Indian Institute of Science Education and Research Thiruvananthapuram, Thiruvananthapuram, Kerala, India – 695551. Email: sukhendu@iisertvm.ac.in

^b Electrochemical Process Engineering (EPE) Division, CSIR-Central Electrochemical Research Institute (CECRI), Karaikudi-630006, Tamil Nadu, India.

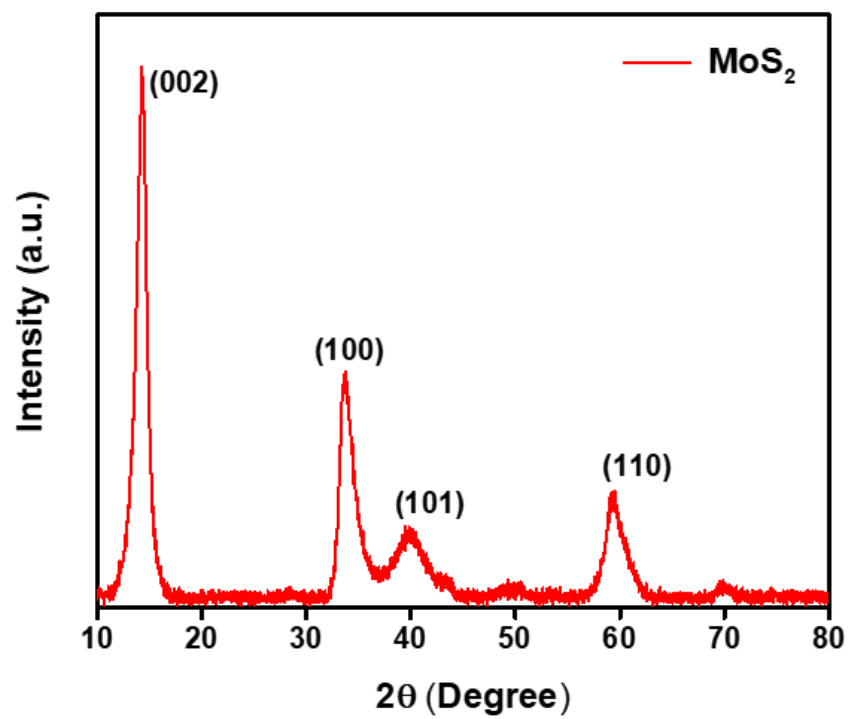
^c Materials Theory for Energy Scavenging (MATES) Lab, Harish-Chandra Research Institute (HRI) Allahabad, HBNI, Chhatnag Road, Jhansi, Prayagraj (Allahabad) 211019 India.

Table of contents

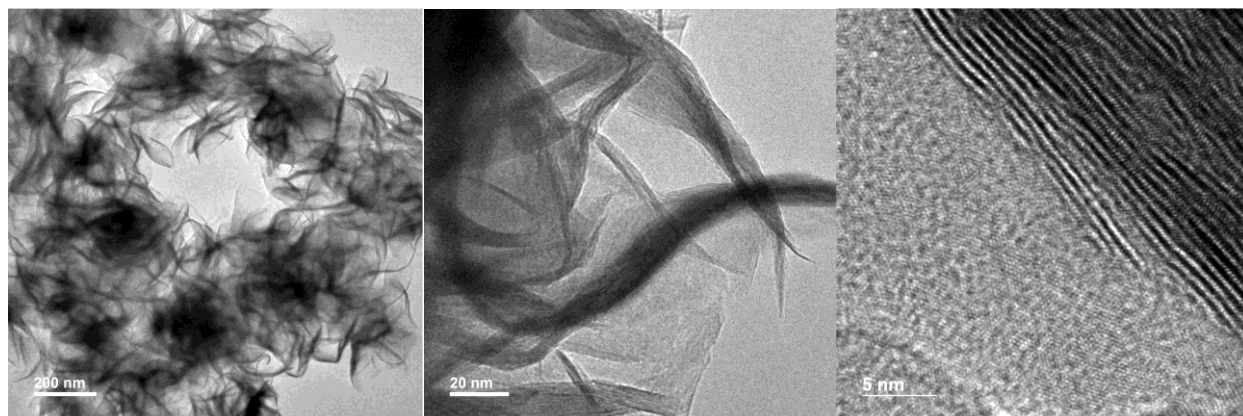
Name	Description	Page No.
Figure S1	PXRD pattern, TEM images and XPS spectra of as-synthesized MoS ₂ nanosheets	3-4
Figure S2	Total crystal structure and UV-vis spectrum of Au ₁₁ (PPh ₃) ₇ I ₃ NC	5
Figure S3	TEM images and the particle size distribution of the Au ₁₁ @MoS ₂ nanocomposites	6-7
Figure S4	XPS spectrum showing the absence of ligands in 2 % - Au ₁₁ @MoS ₂ nanocomposites	7
Figure S5	C _{dl} values, bar diagram for the TOF values calculated at 350 mV overpotential, mass activity plot, EASA normalized polarization curve and chronoamperometric outcomes of the nanocomposites	8
Figure S6	Plots showing the double layer capacitance in the chosen region of non-faradaic region for the nanocomposites	9
Figure S7	PXRD pattern, and XPS spectra of 2 % -Au ₁₁ @MoS ₂ nanocomposite post-HER studies	10-11
	References	12

I. Characterizations

(a)



(b)



(c)

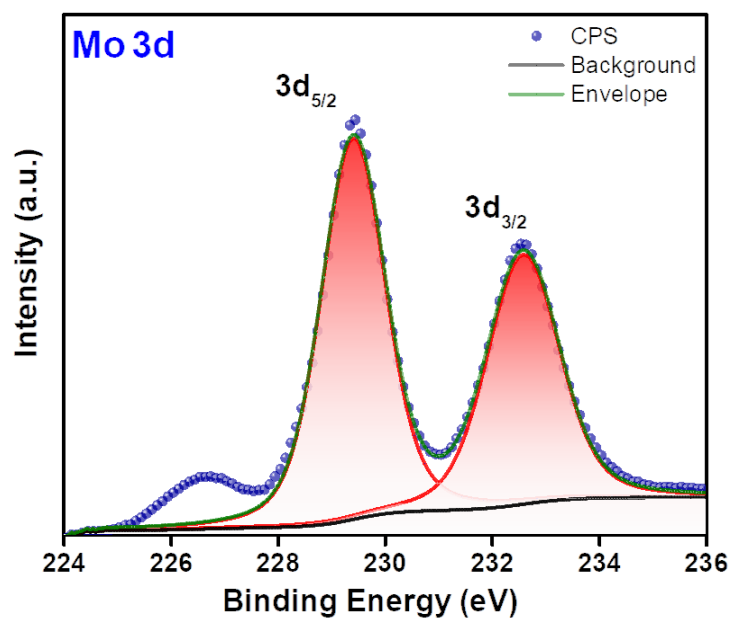
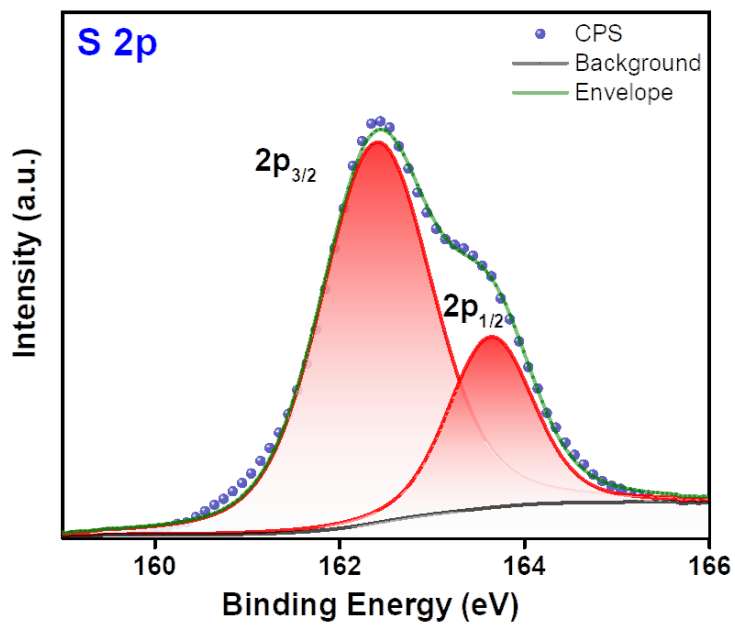
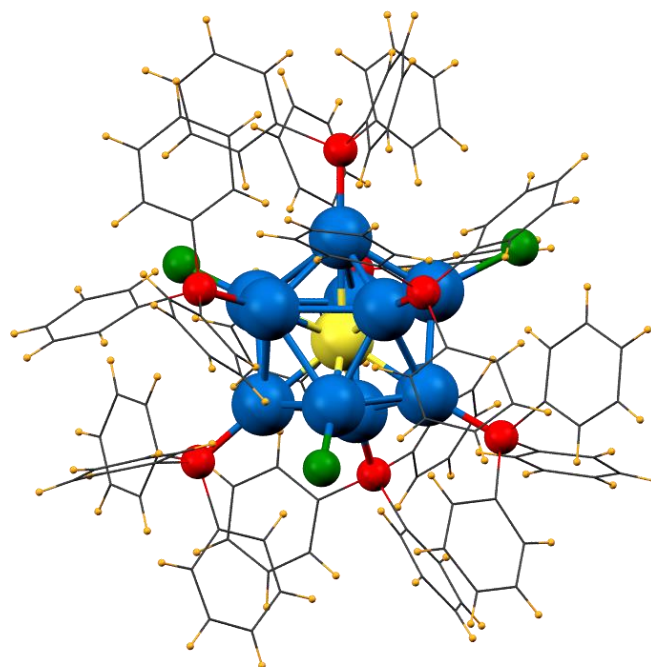


Figure S1. (a) PXRD pattern, (b) TEM images and (c) XPS spectra of as-synthesized MoS₂ nanosheets.

(a)



(b)

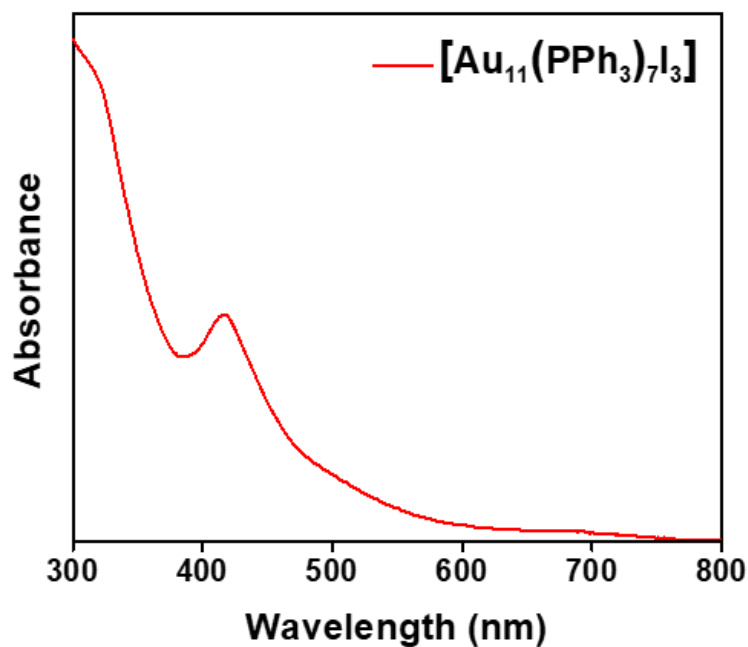
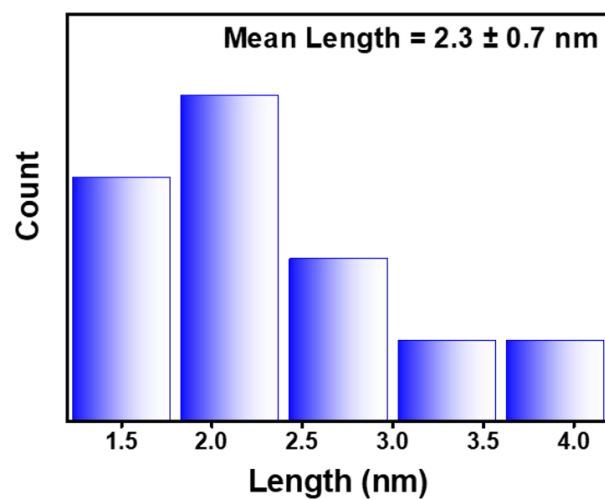
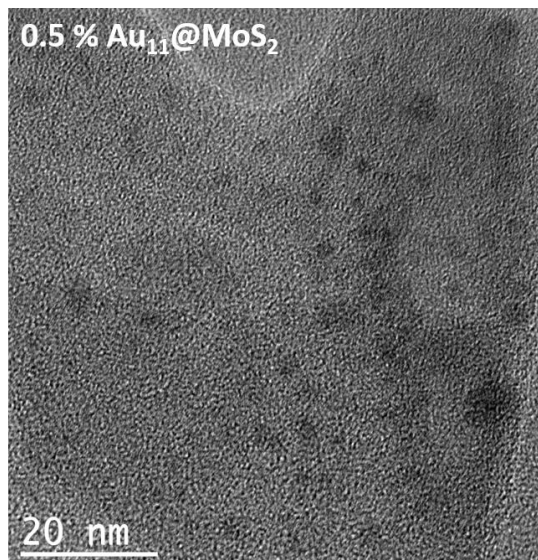
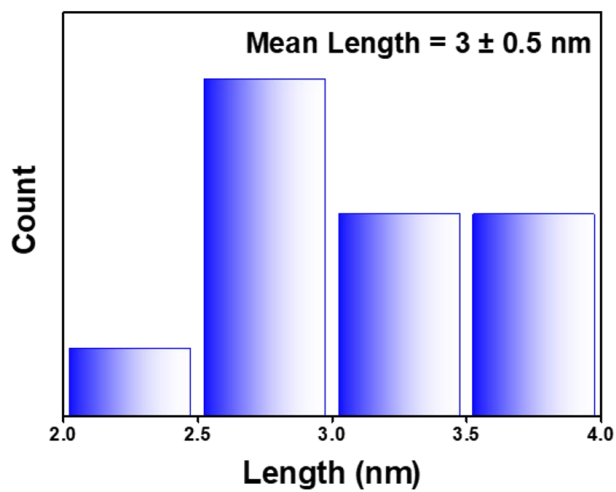
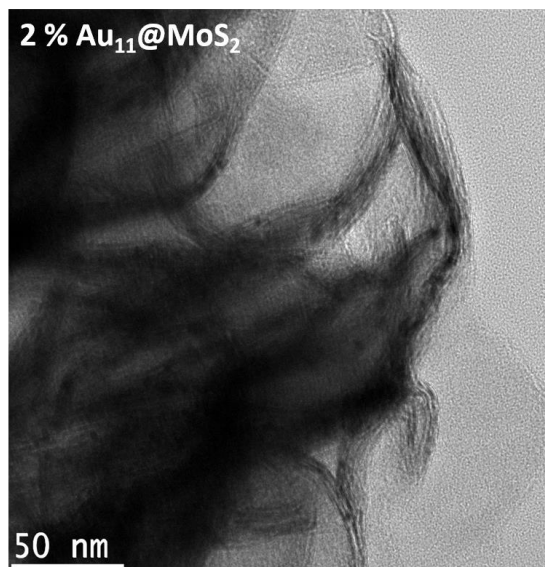


Figure S2. (a) Total crystal structure of Au₁₁(PPh₃)₇I₃ NC. (Color legends: Au, yellow, blue; P, red; I, green; C, gray; H, orange) and (b) The ultraviolet-visible absorption spectrum of Au₁₁(PPh₃)₇I₃ NC in DCM.

(a)



(b)



(c)

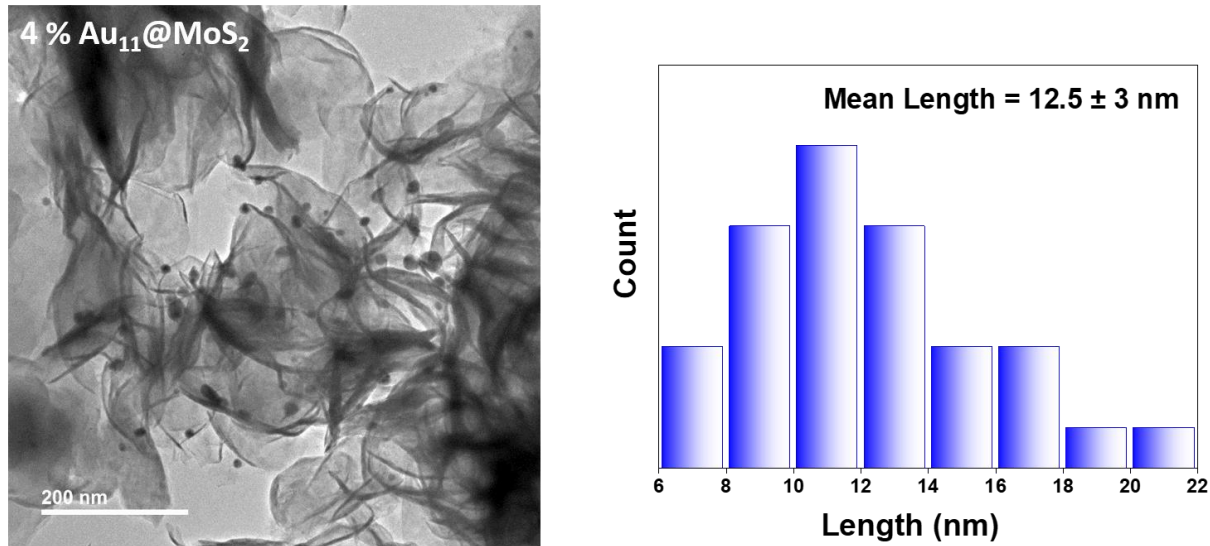


Figure S3. TEM images and the particle size distribution of the (a) 0.5 % - Au₁₁@MoS₂; (b) 2 % - Au₁₁@MoS₂ and (c) 4 % - Au₁₁@MoS₂ nanocomposites.

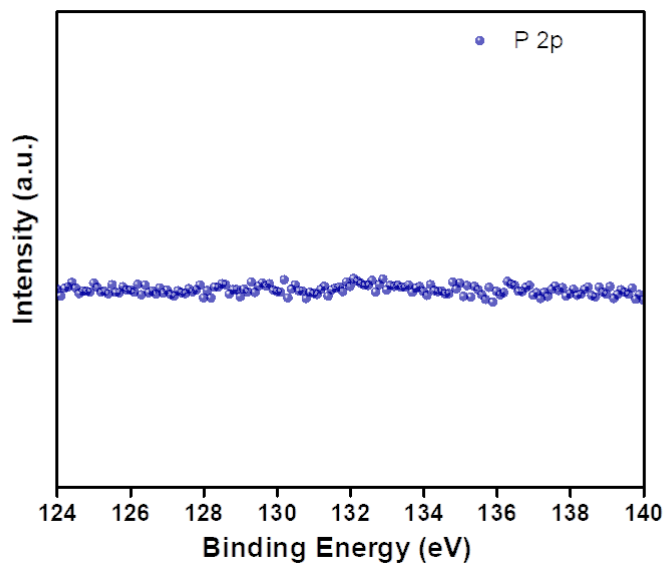


Figure S4. XPS spectrum showing absence of ligands in the 2 % - Au₁₁@MoS₂ nanocomposites.

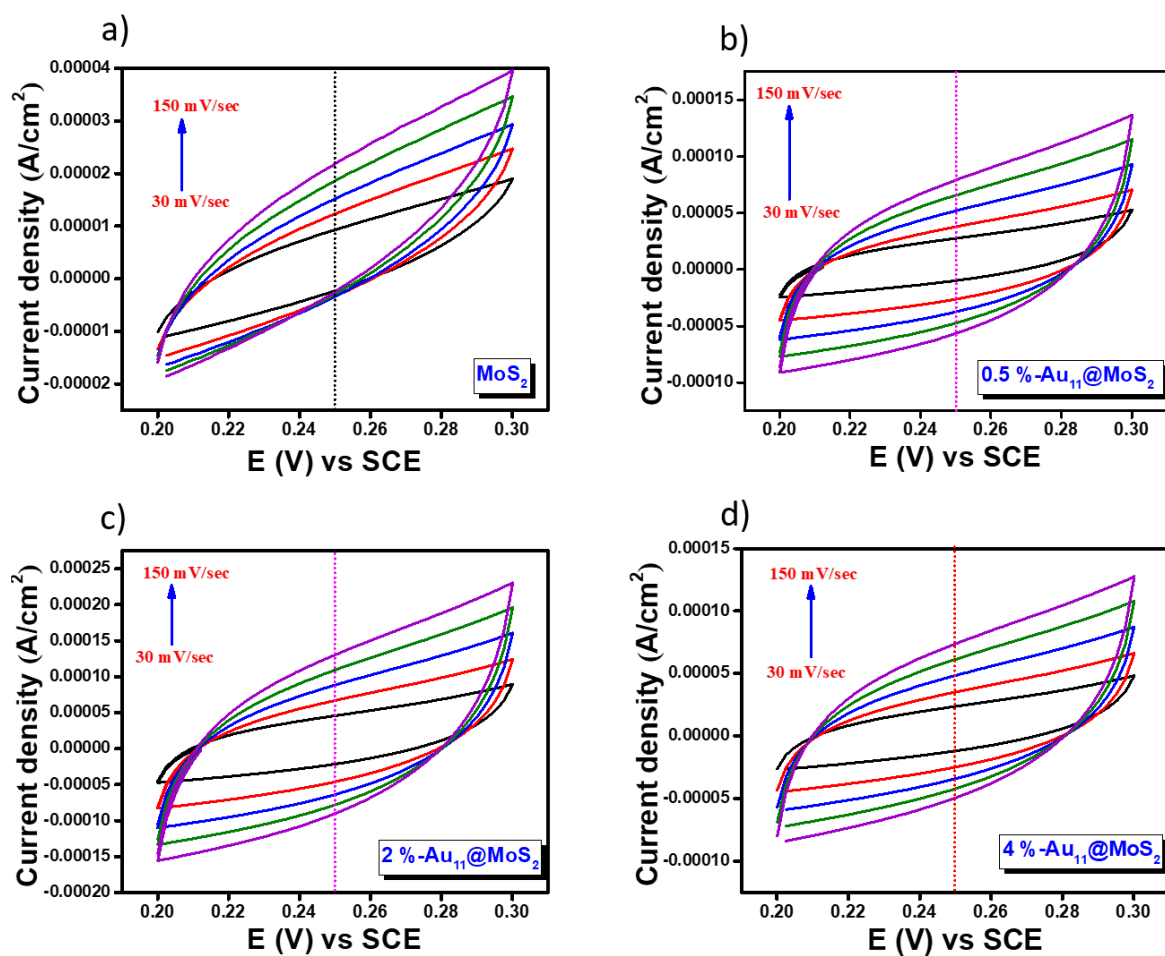


Figure S5: (a-d) is the double layer capacitance in the chosen region of non-Faradaic region for MoS₂, 0.5 % -Au₁₁@MoS₂, 2 % -Au₁₁@MoS₂ and 4 % -Au₁₁@MoS₂ nanocomposites, respectively.

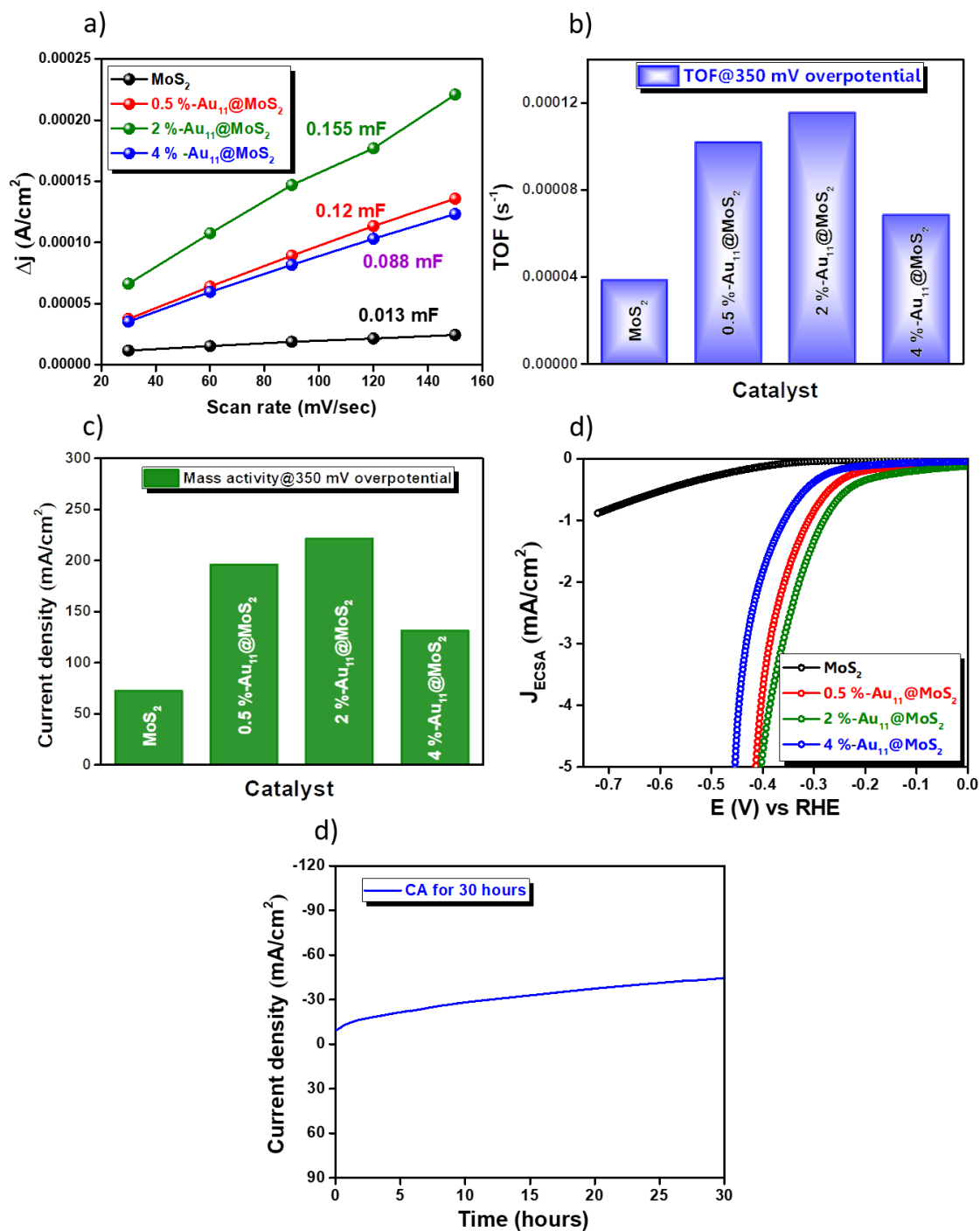
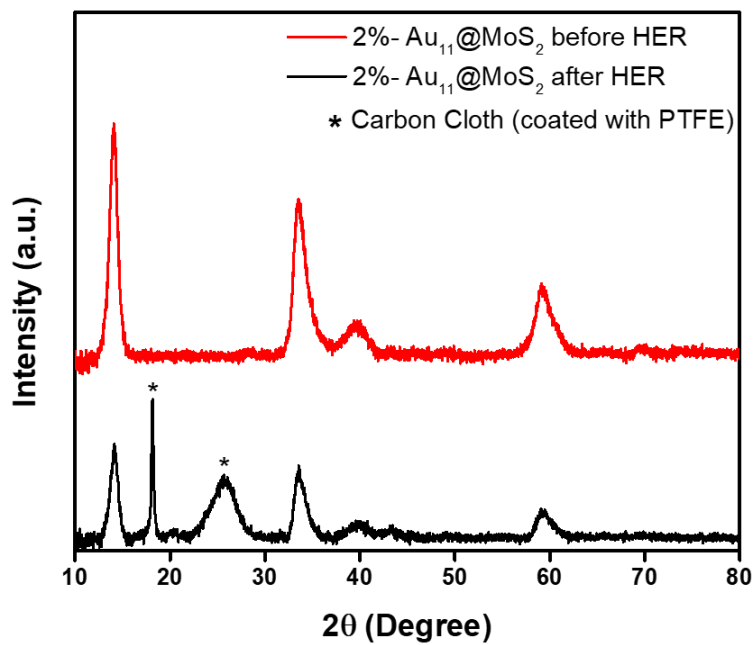


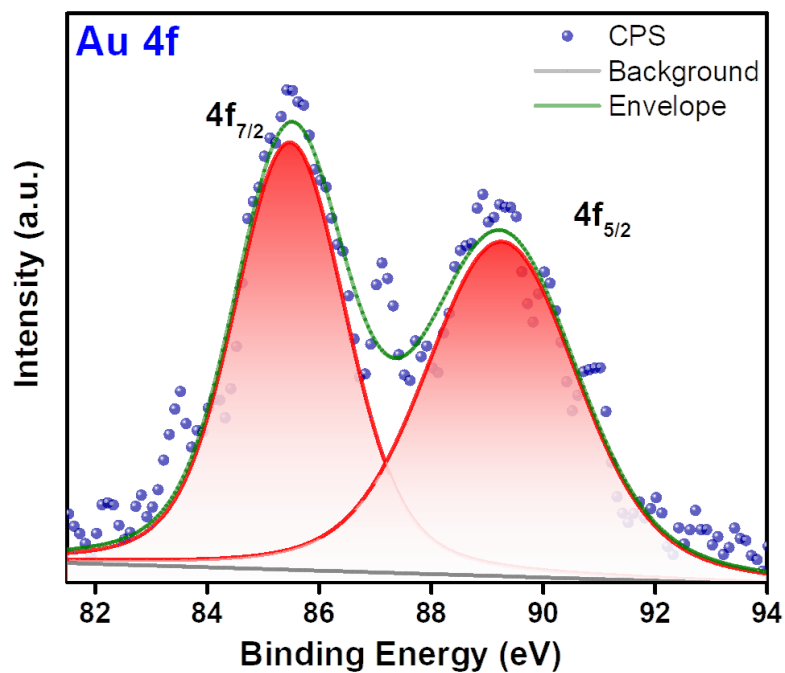
Figure S6. (a) C_{dl} values of all the three catalyst; (b) bar diagram for the TOF values of different catalyst calculated at 350 mV overpotential; (c) mass activity plot for different catalyst; (d) EASA normalized polarization curve and (e) chronoamperometric outcomes.

II. Post-catalytic Characterizations

(a)



(b)



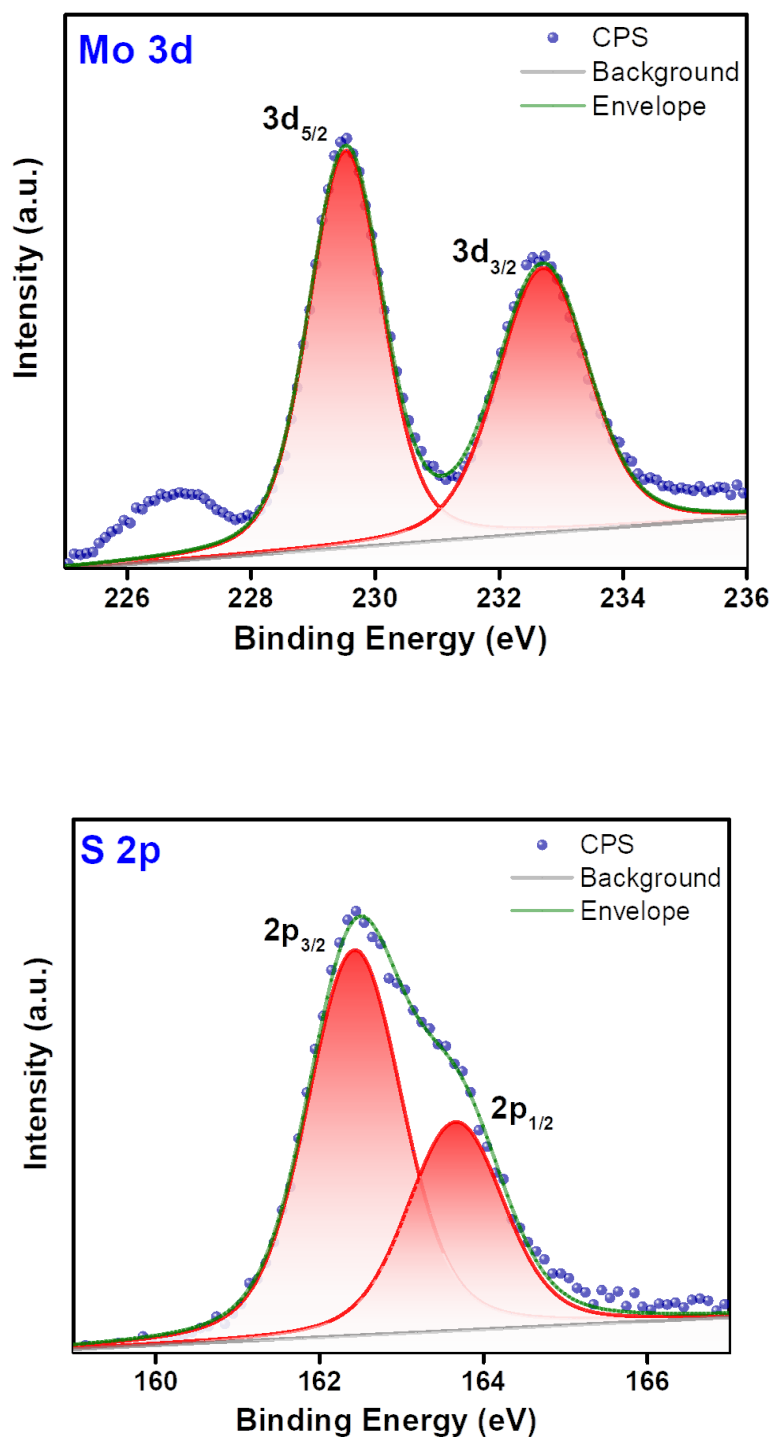


Figure S7. Post-catalytic characterization: (a) PXRD pattern¹ and (b) XPS spectra of 2 % - Au₁₁@MoS₂ nanocomposite after HER-studies.

III. References

1. Warapa Susingrat, Thapanee Sarakonsri, Nutpaphat Jarulertwathana, Jaron Jakmune, Khac Duy Pham and Chung Hoeil, *Journal of Materials Science and Engineering A*, 2017, **7**, 178-187.